2021-02

A numerical investigation of the sealing performance and the strength of a raised face metallic bolted flange joint

Aljuboury, M

10.1016/j.ijpvp.2020.104255
International Journal of Pressure Vessels and Piping
Elsevier BV

A numerical investigation of the sealing performance and the strength of a raised face metallic bolted flange joint

Muhsin Aljuboury[1,2], Md Jahir Rizvi[2], Stephen Grove[2], Richard Cullen[2]
[1]School of Civil Engineering, Al-Qalam University College, Kirkuk, Iraq
[2]*School of Engineering, Plymouth University, Plymouth, UK*
Corresponding author:
Email: muhsin.aljuboury@plymouth.ac.uk
muhsin.aljuboury@alqalam.edu.iq

Abstract

The development of leakage and strength of a metallic bolted flange joint are investigated in this work. Finite element analyses in 2D and 3D have been developed using ANSYS to study a steel flange and bolt with an aluminium gasket. The pressure-penetration criterion (PPNC) in ANSYS has been used to model fluid leakage propagation between the flange and the gasket. Validation was performed with a benchmark test, using published study of a bolted metallic flange joint; the agreement between the results is excellent. Results showed that the finite element method using PPNC is a good method to study leakage behaviour compared to other methods, which are relatively time-consuming and expensive. The influence of the flange dimensions on the maximum stresses and leakage propagation has been investigated in this study. Furthermore, the agreement between the 3D and axisymmetric 2D FEA models is very good, so the latter can be used to save computational time. This study was undertaken as a preliminary to a larger project about bolted flange joints made of composite materials.

Keywords: Bolted flange joint; Sealing performance; Fluid pressure penetration; Flange rotation

Nomenclature

A_i	Internal area of the pipe
A_k	Cross section area of pipe wall
FPP	Fluid pressure penetration
FT	Flange thickness
GFRP	Glass fibre reinforced polymer
H_D	Hydrostatic end force
P	Internal pressure
P_k	Axial component of the internal pressure
PPNC	Pressure-penetration criterion
U_θ	Circumferential displacement
U_z	Axial displacement
HTB	Hub thickness at bottom

1. Introduction

Bolted flange pipe connections are widely used in many industries such as chemical, power plants, petrochemical and offshore oil and gas industries. This is because the systems in these industries usually include pumps, valves and other fittings that require periodic removal for maintenance. So far, many investigations have been carried out onto the characteristics of bolted flange connections to tackle the several issues related to the actual ASME flange design code procedure [1] and other standards that have been established based on the earlier work of Waters et al. [2] and is known as Taylor Forge method [3, 4]. In addition, several studies investigated the issues of the gasket and the sealing performance, which is governed by the distribution of the contact stress that is caused by the bolt axial load. However, fluid pressure penetration (FPP), which is produced as a result of applying fluid pressure between the flange and the gasket, has not been investigated sufficiently for the raised face gasket flange joint.

The purpose of this study is to investigate joint sealing performance using the pressure penetration criteria PPNC in ANSYS for a raised face of a metal bolted flange joint, which has been studied experimentally and numerically by Sawa et al [5]. This study was undertaken as a preliminary to a larger project about bolted flange joints made of composite materials, which has been published partially in these references [4, 6-10].

2. Literature review

During the last three decades, many studies have been conducted on the sealing performance between the flange and the gasket. Krishna et al [11] had carried out a comparison of the gasket's influence on the sealing performance of a bolted flange. A three-dimensional FE model of bolted flange connections with gaskets has been developed and analysed using ANSYS. Spiral wound gaskets with various filled such as; asbestos (AF), graphite (GF) and PTFE (TF) filled have been used with their nonlinearity characteristics obtained from experiments. The results show that the distribution of the contact stress is non-uniform in the radial direction across the gasket width and depends on both the gasket type and the flexibility of the flange. These factors are not accounted by the ASME code, so the leakage may occur even at the flange rotation of less than 3° that is specified by ASME. The highest and the lowest axial bolt force have been observed with TF and GF gaskets respectively when the internal pressure is increased. This is due to low and high stiffness of TF and GF gaskets

respectively. It is also apparent from the results that the TF spiral wound gasket has the least variations in the contact stress distributions whereas the GF spiral wound gasket has an opposite trend.

Shoji and Nagata [12] presented FE analysis of a raised flange with nonlinear gasket using a 2-D axisymmetric and 3-D solid element FE models. This type of flange was described in article [4]. Based on the load condition, the analysis has been carried out in two steps pre-load and pressurized. Due to the nonlinearity of the gasket, they have used two values of modulus of elasticity (compression and decompression) depending on the states of the gasket whether in compression or decompression. Results of the numerical simulations indicate that the gasket stress increased from the inner radius toward the outer radius of the gasket for both the 2-D and the 3-D models, and the stresses are higher in pre-load conditions than in pressurized conditions.

Aljuboury et al [6] have conducted a numerical investigation of a sealing performance of a bolted glass fibre reinforced (GFRP) bolted flange joint with rubber gasket. The FEA model, which was developed by using ANSYS, has taken into account the orthotropy of the GFRP materials and the non-linear behaviour of the rubber gasket material for both the loading and non-loading conditions. In addition, the pressure-penetration criterion PPNC in ANSYS has been used to model the leakage propagation between the flange and the gasket. The results show that the minimum contact pressure is found at the inner radius of the gasket and increases in the radial direction. Also in the circumferential direction, the contact pressure at the bolt hole is larger than at the midpoint between the bolts. For the distribution of the fluid pressure penetration (FPP) between the flange and the gasket, the results indicate that the leakage development has started at the inner radius of the gasket, where the contact pressure is lower than other places, and grows towards the outer radius. Also, due to uneven distribution of the bolt loads in the circumferential direction, the leakage growth at the midpoint between the bolts is more than at the bolt centre.

3 . Scope of work

In this paper, a previous study, which was conducted by Sawa et al [5], has been used to validate the FEA analysis; the authors used an axisymmetric three-dimensional theory of elasticity to study the contact stress distribution. Numerically, the influences of the material stiffness and the thickness of the gasket on the contact stress distribution have been

investigated. Furthermore, the hub and bolt stresses as well as the load factor are studied. The results showed that the leakage pressure took place experimentally at 16.5 MPa whereas numerically at 12.25 MPa when the bolt load is 15 kN.

As shown earlier, most of authors focus on the average of the contact stress between the flange and the gasket to predict the leakage pressure whereas this study predicates the leakage by simulating the fluid pressure penetration using ANSYS and PPNC criterion, which achieved a good accuracy. In this method, a comparison is conducted between the values of the internal fluid pressure and the contact stress (pressure) for each element starting from the elements that in direct contact with the fluid then to the adjacent elements. This will encourage the researchers to use the FEA more for predicating the leakage in the bolted flange joint rather than the experimental test, which is expensive and requires too much time.

4. Flange joint geometry and material properties

4.1 Geometry of the flange, gasket and bolt

Fig.1 shows a section of the geometry and the dimensions of the raised face flange joint, compliant with standards JIS B (Japanese International standard) and ANSI B 16.5 (American standard). The joint includes two pair flanges, gasket and eight bolts. The joint has been investigated experimentally by Sawa et al [5].

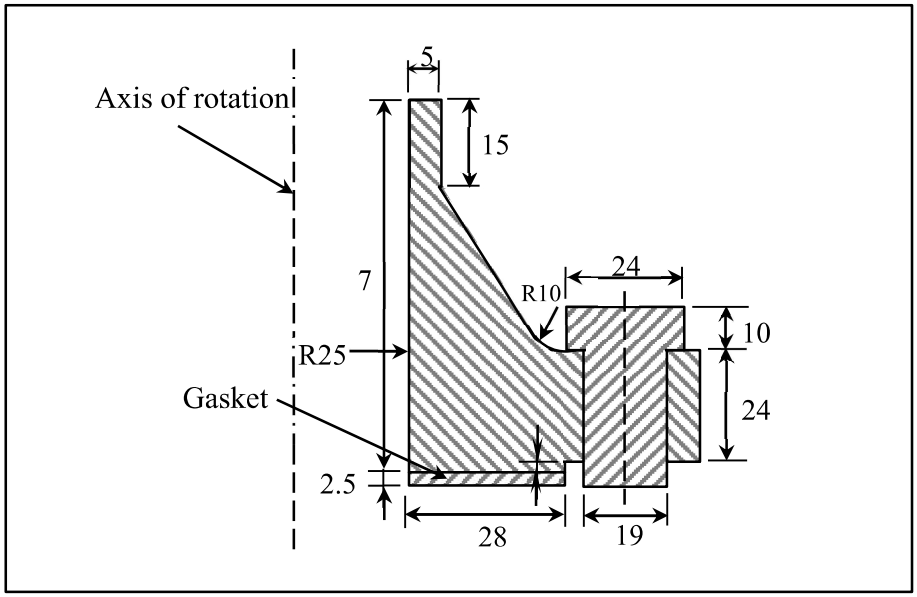

Fig. 1: Raised face bolted flange joint (All dimensions in mm)

4.2 Material properties

The materials of the flange, bolt and gasket are assumed to be homogenous, isotropic and linearly elastic. The flange was made of steel (S45C, JIS), with $E = 206\ GPa,\ v = 0.3$, and the bolts are chromium molybdenum steel (SCM435, JIS), with $E = 206\ GPa,\ v = 0.3$. Aluminium (AI-H, JIS) was selected to make the gasket with $E = 68.7\ GPa,\ v = 0.3$.

5. Finite Element Analysis (FEA)

5.1 3D solid element model

A three-dimensional finite element model has been developed for the bolted flange using ANSYS v18. The model includes flange, gasket and bolt. Using symmetry, a primary segment is repeated at equally spaced intervals about the axis of symmetry; $1/16^{th}$ portion of the total circumference of the joint has been considered as shown in Fig. 2. This option has been chosen to reduce the total simulation time and computer resources.

5.1.1 Element selection and contact interfaces

Several different elements are used in the FEA study of the flange joint. For the flange, solid structural elements (SOLID186) are used. At the contact zones, CONTA174 and TARGE170 elements are utilized to simulate the contact distribution between the lower face of the flange and the gasket surface, the top face of the flange and the bolt head. These elements are compatible with structural element SOLID186 [13]. Since the behaviour of the flange, the gasket and the bolt are different in terms of the load-deformation characteristics, and all of them are deformable, they are treated as a 'flexible-to-flexible' category and the contact surfaces between them are modelled as 'frictionless'. Because the gasket is softer than the flange, it is simulated as a contact surface and the flange is modelled as a target surface [14]. In contrast, the flange is simulated as contact and the bolt as a target in their contact interface.

5.1.2 Boundary conditions

As mentioned earlier, due to the rotational symmetry and also due to the symmetry about the plane that passes through the gasket mid thickness, the boundary conditions and the loads are applied to an upper single segment in the analysis. For the model created in the cylindrical coordinate system, the circumferential displacements in the normal direction on the surface of the cycle symmetry are assumed as fixed, i.e. $U_\theta = 0$. Also, the displacements of elements

located at the bottom surface of the gasket are fixed, i.e. U_z=0. These boundary conditions are assigned for both bolt-up and pressure stages, which will be discussed in the next sections.

5.1.2.1 Bolt preload condition

Initially, a bolted flange connection system is analysed to obtain the initial stress and deformation during the seating condition when the initial clamping force is applied during assembly. In this stage, the gasket is subjected to compressive pressure that deforms the gasket to fill the irregularities on the flange face, ensuring full contact over the surfaces. To achieve this initial stress value in the FE model, the bolt pre-load force is applied to the lower bolt surface.

5.1.2.2 Pressure loading condition

This research models the bolted flange system under combined bolt pre-load and internal pressure, to study the stress and the deformation, and to investigate the sealing performance. Hydrostatic end force and pressure induced on the joint system as well as the bolt load have been applied in the initial clamping phase. The hydrostatic end force is calculated from the inner pipe diameter:

$$P_k = \frac{A_i}{A_k} P \qquad \ldots (1)$$

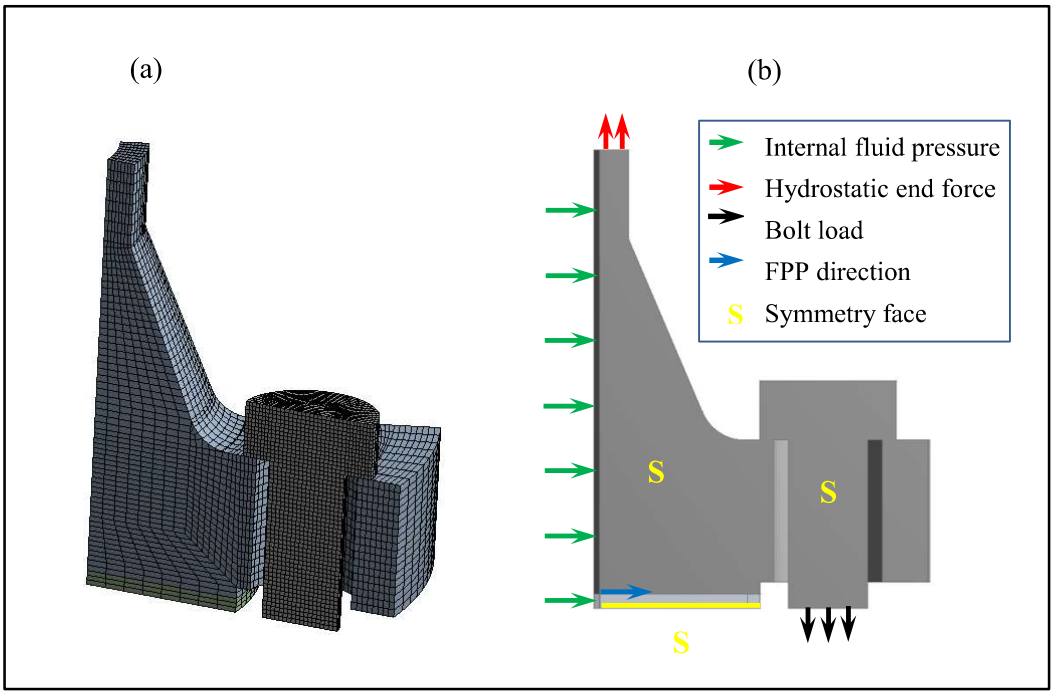

Fig. 2: (a) 3D model flange joint with mesh (b) Boundary conditions

5.1.3 Modelling leakage development

The fluid pressure penetration (FPP) between the flange and the gasket is modelled in ANSYS by a pressure-penetration criterion using the contact element real constant PPCN. Based on the comparison between the internal pressure and the contact stress between the flange and the gasket, the fluid can penetrate new areas between the contact surfaces starting from the elements that are in direct contact with the internal fluid. For example, when the contact stress is less than the fluid pressure, the penetrating fluid starts to penetrate from the starting points (radially) towards the outside. In contrast, when the contact stress is greater than the fluid pressure, the penetrating fluid returns back to the starting point; that is, fluid penetration is cut off [13]. Therefore, since the contact pressure between the flange and the gasket decreases and the separation progresses as a result of the boundary conditions, the internal pressure is applied to the separated elements to induce more load on the joint system. Due to symmetry, two edges have been specified as closed edges to prevent the fluid from entering. This feature of fluid pressure penetration capability has been added from version 12.0 of ANSYS [15].

5.2 2D FEA axisymmetric models

The 2D FEA of the joint has been generated using ANSYS with element PLANE183 for the flange and the gasket, and element CONTA172 for the contact region between them. The mesh of this model is shown in Fig. 3. As with the 3D FEA, the boundary conditions have been applied into two steps: during the first step (bolt up load stage), the axial displacement at the lower edge of the gasket has been fixed due to the axial symmetry at the mid-thickness of the gasket. The axial bolt load has been converted to the equivalent pressure force which has been applied on the flange area under the bolt head. In the next step, the fluid pressure has been applied on the internal surface of the flange and the gasket. In addition, the axial pressure components of the hydrostatic pressure force have been applied to the top edge of the flange. The leakage propagation between the flange and the gasket has been simulated by using PPNC criterion.

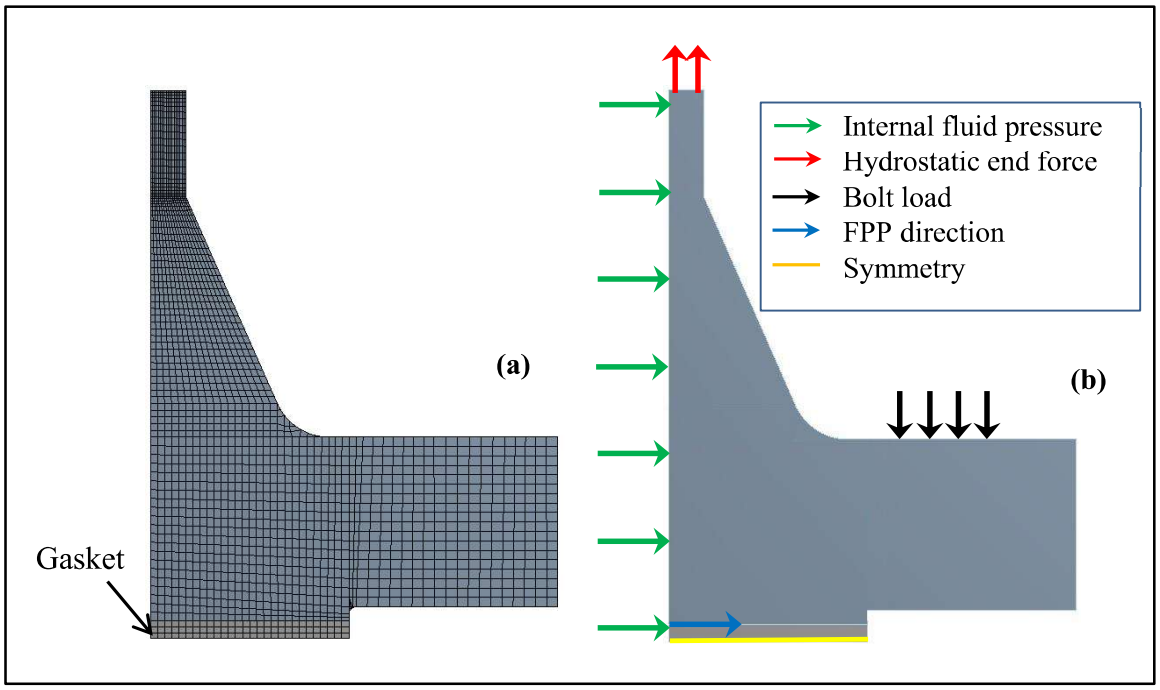

Fig. 3: (a) 2D FEA model flange joint with mesh (b) Boundary conditions

6. Results and discussion

The results presented in this paper are obtained from the FEA models (3D and 2D axisymmetric) under bolt up and working conditions when the bolted flange joint is subjected to between 10 to 17 kN bolt load and the internal pressure is increased up to the leakage point.

6.1 FEA Validation

In order to validate the FEA of this study, the results have been compared with a metallic bolted flange joint that has been investigated experimentally and numerically by Sawa et al [5]. The hub stress (axial stress) has been measured at the outer bottom surface of the hub and near the bolt. The agreement between the results is excellent for the hub stress and the leakage point, as shown in Fig.4. In this study, the leakage pressure occurred at 14.05 MPa for the 3-D FEA and 13.87 for 2-D FEA whereas for the other study [5], the leakage pressure occurred at 16.5 MPa for the experimental test and 12.25 MPa for the numerical model. This confirms the high performance of the developed FEA model with using PPNC criterion to predict the leakage pressure, which needs long-time and high cost to be found experimentally.

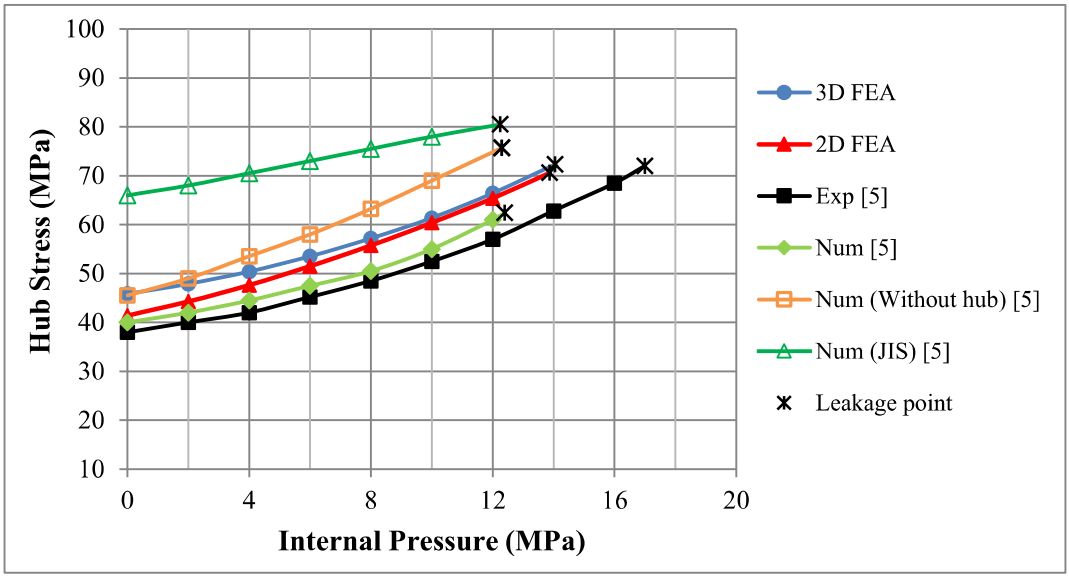

Fig. 4: Flange hub stress variation with the internal pressure up to leakage point

6.2 Total deformation

Fig. 5 shows the total deformation of the joint obtained from 3D and 2D FEA. The maximum and minimum total deformation of both cases occur at the same points on the flange body. Also, the maximum deformation is observed at the outer diameter of the flange, due to the flange rotation as a result of the bending forces.

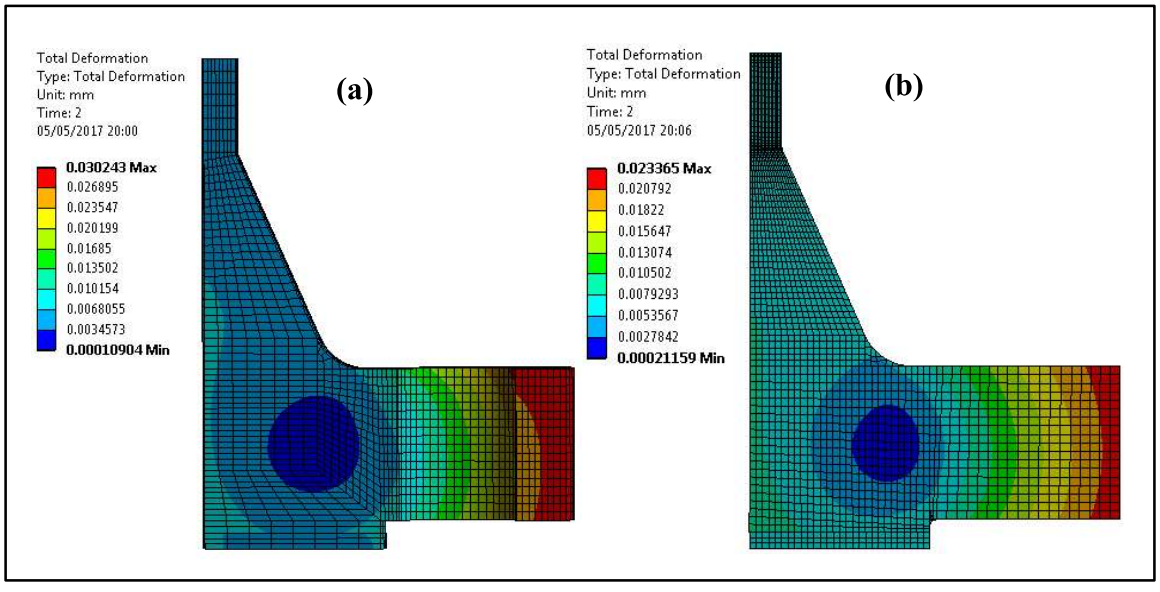

Fig. 5: Total deformation of the flange joint (a) 3D FEA (b) Axisymmetric (2D FEA)

6.3 Flange-gasket contact pressure

The distribution of the contact pressures on the top gasket surface is illustrated in Fig. 6. The results show that the minimum contact pressure is found at the inner radius of the gasket, which is in direct contact with the internal pressure of the fluid, and increases in the radial direction. Also in the circumferential direction, the contact pressure at the midpoint between the bolts is larger than at the bolt hole. This due to the flange geometry and the boundary conditions, bolt loads, internal pressure, hydrostatic end force and total hydrostatic force, which all produce a bending moment and hence flange rotation.

Fig. 7 shows the variation of the maximum contact pressure found at the midpoint between bolts, with bolt load and internal pressure up to the leakage point. The results reveal that the contact pressure increases as the bolt load increases and decreases when the internal pressure increases.

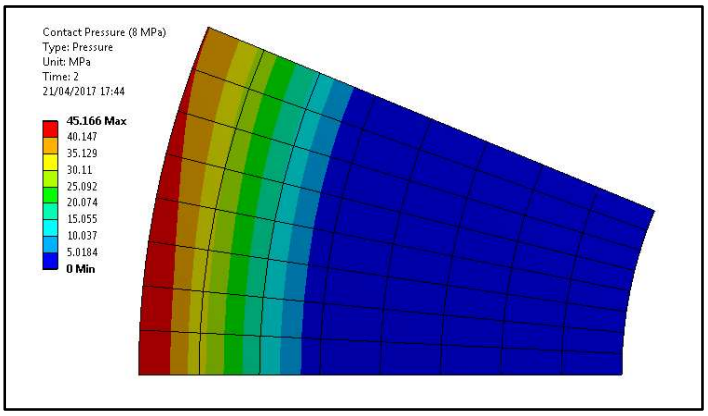

Fig. 6: Distribution of contact pressure on gasket

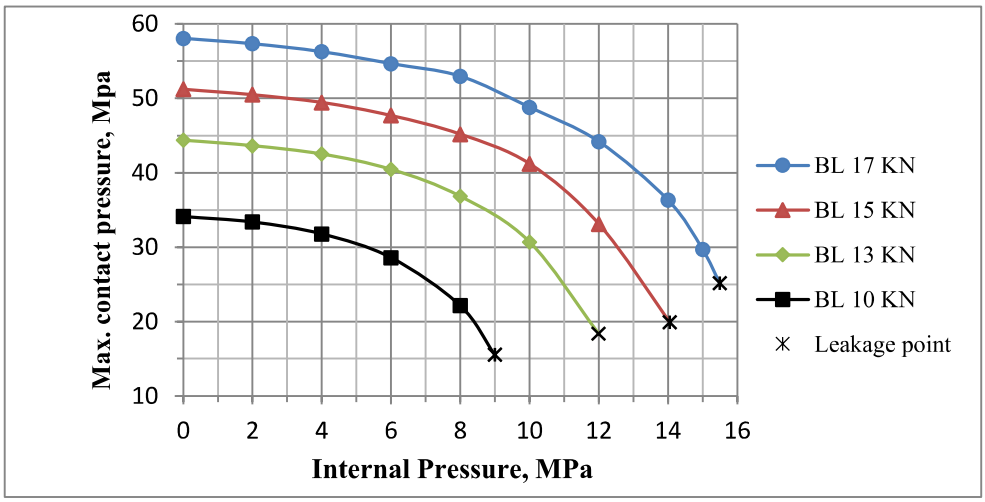

Fig. 7: Variation of maximum contact pressure on gasket with internal pressure and bolt load (BL) of 3D FEA

The rate of decrease of the contact pressure at higher pressures is more than at lower pressures because of leak growth, and more area of the flange and gasket has been subjected to the fluid pressure. In other words, the area subjected to the fluid pressure penetration at any point after the leakage starts is bigger than that at the beginning of the leakage growth as well as the value of the pressure itself.

6.4 Leakage development

Fig. 8 represents the leakage propagation in 3D FEA during the operating conditions with bolt load of 15 kN. It is found that the leakage grows radially as the internal pressure increases and the leakage occurs at a pressure of 14.05 MPa. Similarly, Fig. 9 shows the leakage development in the axisymmetric model when the flange joint is pressurized. In this FEA the leakage point has taken place when the internal pressure has reached 13.87 MPa. It is clear that the agreement between two models is very good. The relationship between the bolt load and the internal pressure at the leakage has been investigated using both 2D FEA and 3D FEA as shown in Fig. 10. It is observed that the relationship between them is linear and there is an excellent agreement between two models, so the 2D FEA axisymmetric can be used to save computational time.

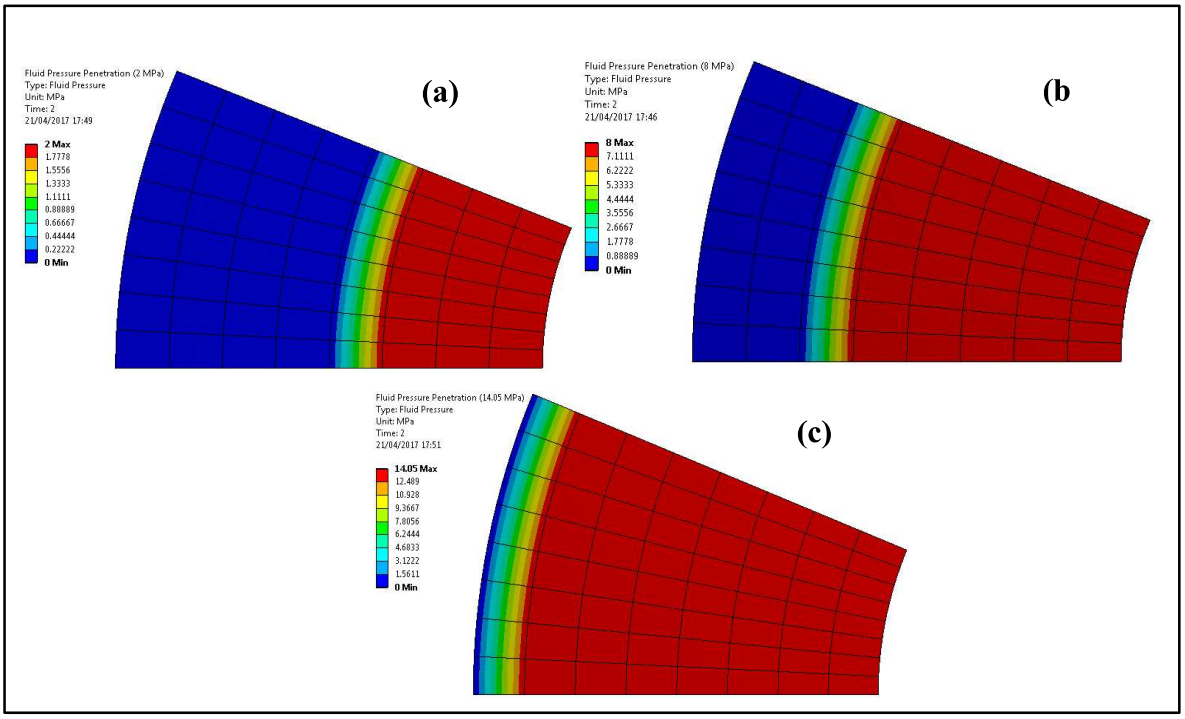

Fig. 8: Fluid pressure penetration on the gasket contact surface of the 3-D FEA (a) Internal pressure 2 MPa (b) Internal pressure 8 MPa (c) Internal pressure 14.05 MPa (Leakage point)

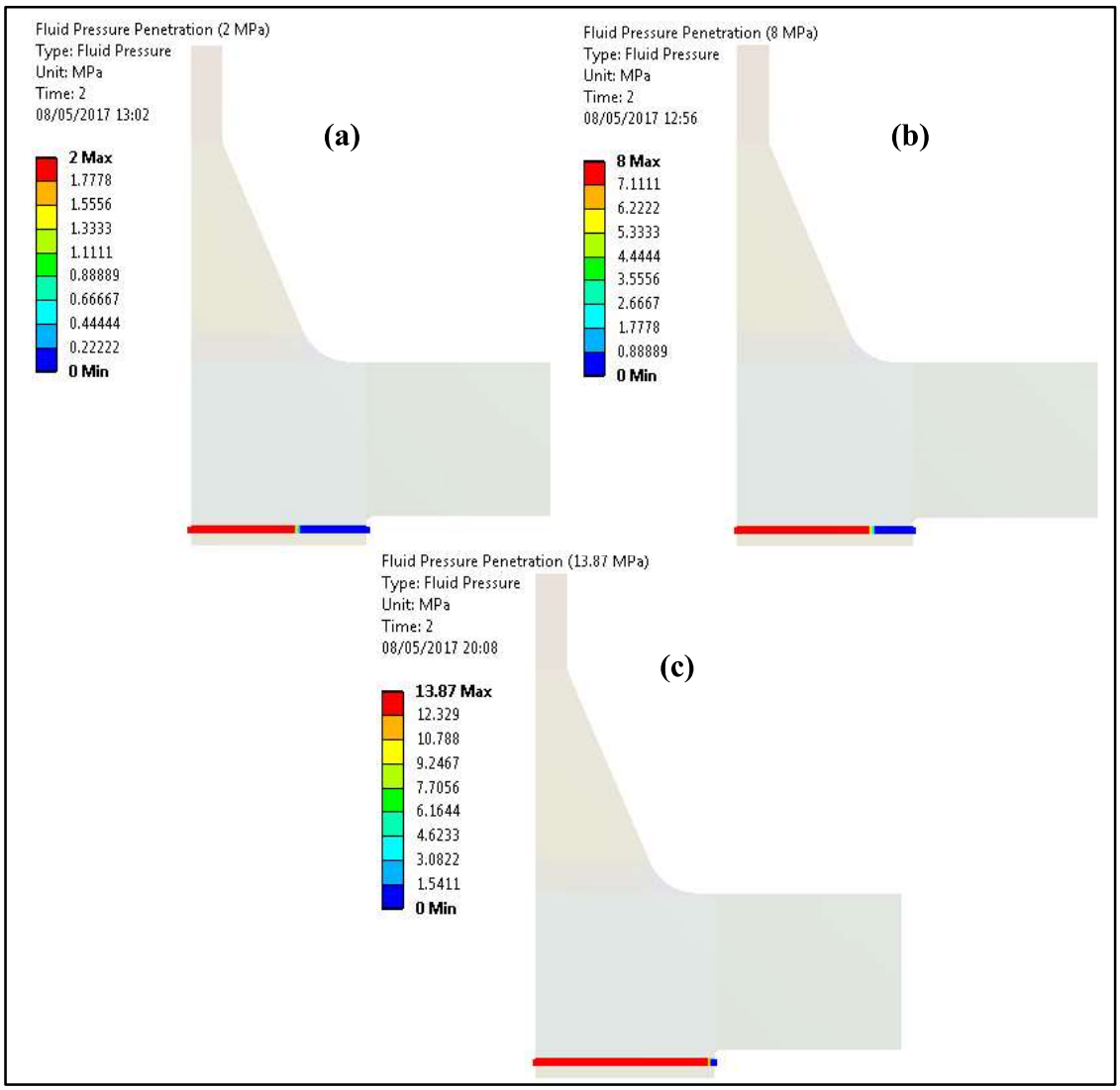

Fig. 9: Fluid pressure penetration on the gasket contact surface of the 2-D FEA (a) Internal pressure 2 MPa (b) Internal pressure 8 MPa (c) Internal pressure 13.87 MPa (Leakage point)

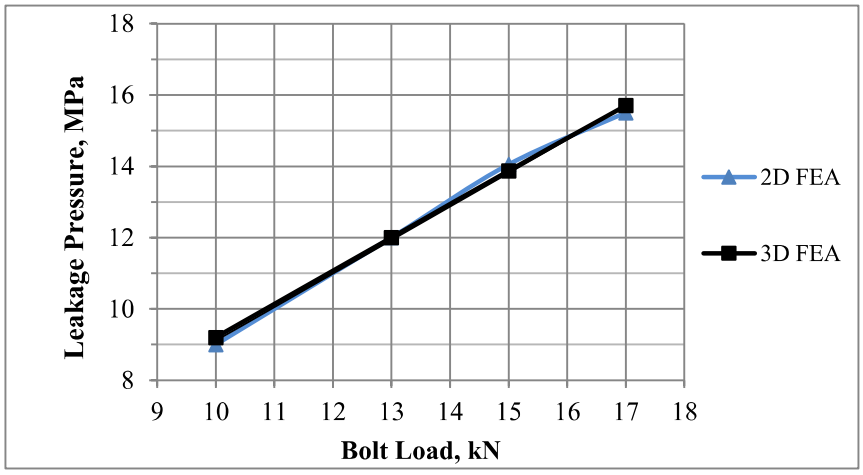

Fig. 10: Variation of the leakage pressure with the bolt load

6.5 Flange rotation

Tight sealing requires sufficient contact stress between the flange and the gasket. This contact stress is produced by tightening the bolts of the joint, which lead to deformation of the gasket. Due to the eccentricity of the bolts pre-load, sealing contact surface (reaction load of the gasket), internal pressure on the inner flange face and hydrostatic end force (H_D), a bending force is produced and causes a flange rotation. This leads to an uneven compression load, which has a significant effect on the sealing performance. Fig. 11 shows the relationship between the flange rotation, which has been calculated using 3D FEA and based on the axial displacements, and the internal pressure load up to the leakage point at various bolt loads from 10 to 17 kN on the bottom face of the flange that is in direct contact with the gasket. As shown in the figure, the flange rotation increased with increasing internal fluid pressure and the bolt pre-load. It is observed that the flange rotation is slightly non-linear and the influence of the bolt load on the leakage point at high pressure is less than at the lower values of the pressure. The flange rotation has been calculated using 2D FEA up to the leakage point, and compares very well with results of 3D FEA (Fig. 12).

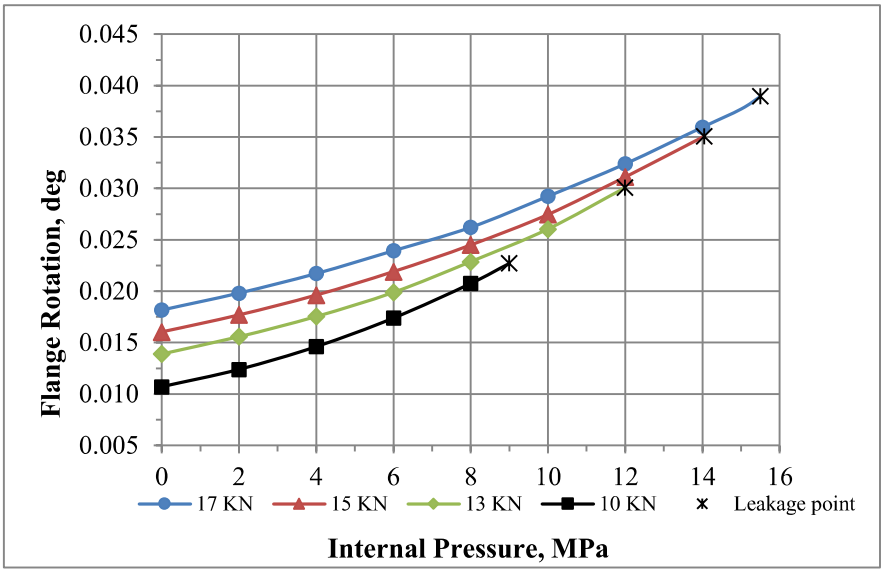

Fig. 11: Variation of flange rotation with internal pressure

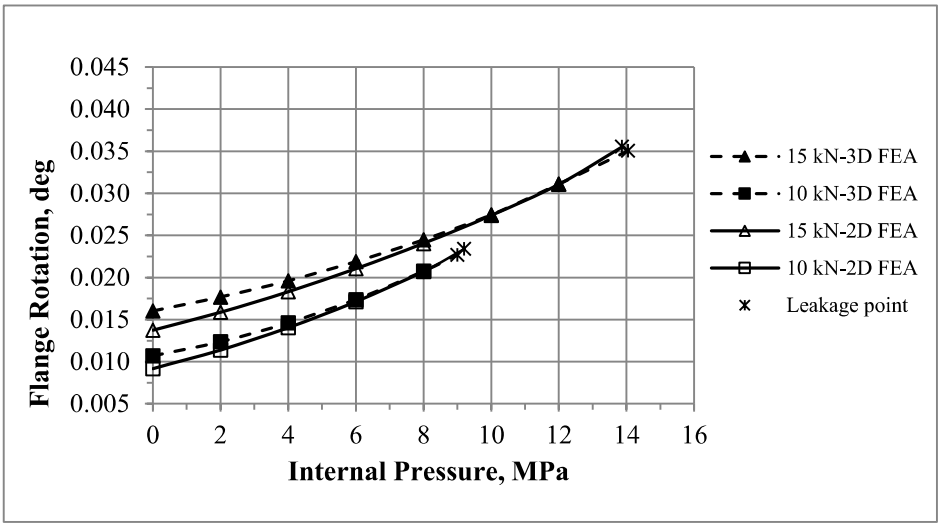

Fig. 12: Comparison of 2D and 3D FEA for flange rotation with internal pressure under different bolt load

6.6 Axial displacement

The relationship between the flange axial displacement and the radial distance as well as the internal pressure has been modelled in 3D FEA (Fig. 13). The displacement is calculated at the lower face of the flange along the radial line that passes through the centre line of the bolt. The findings reveal that the maximum axial displacement occurred at the internal diameter of the flange and decreased gradually towards the outer diameter. In addition, its values are affected significantly by the internal pressure, especially at high pressures.

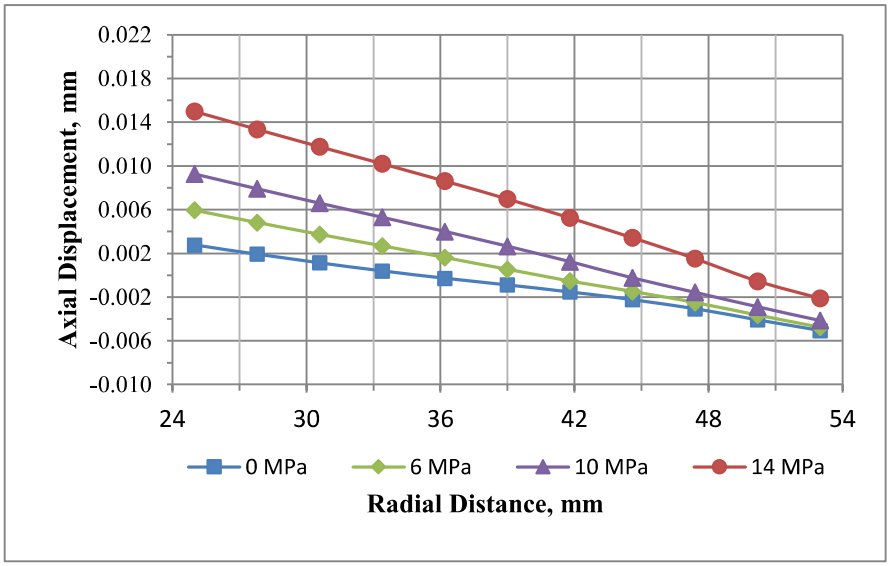

Fig. 13: Variation of flange axial displacement with the radial distance

6.7 Flange thickness effect

In this section and the next section, a parametric study has been conducted to investigate the relationship between the flange geometry (flange thickness and hub thickness) and the leakage pressure and the maximum axial, hoop, radial stresses using 2D and 3D FEA. The bolt load is 15 kN and the internal pressure is 8 MPa. In this section, the flange thickness has been varied from 24 mm, which is recommended by the standards JIS B and ANSI B 16.5, to 16 mm.

Maximum axial stress vs flange thickness, Fig. 14 illustrates the maximum axial stress variation with the flange thickness using 2D and 3D FEA. The maximum stress has been found at the outer surface of the hub near the bolt. It is observed that decreasing the flange thickness (24 to 16 mm) leads to increase the maximum axial stress. This occurs because of the decreasing in the bending resistance of the flange, which becomes more flexible. This produces more axial stress at the flange-hub intersection because of applying the bolt force and the internal pressure. The agreements between the 2D and the 3D FEA is excellent.

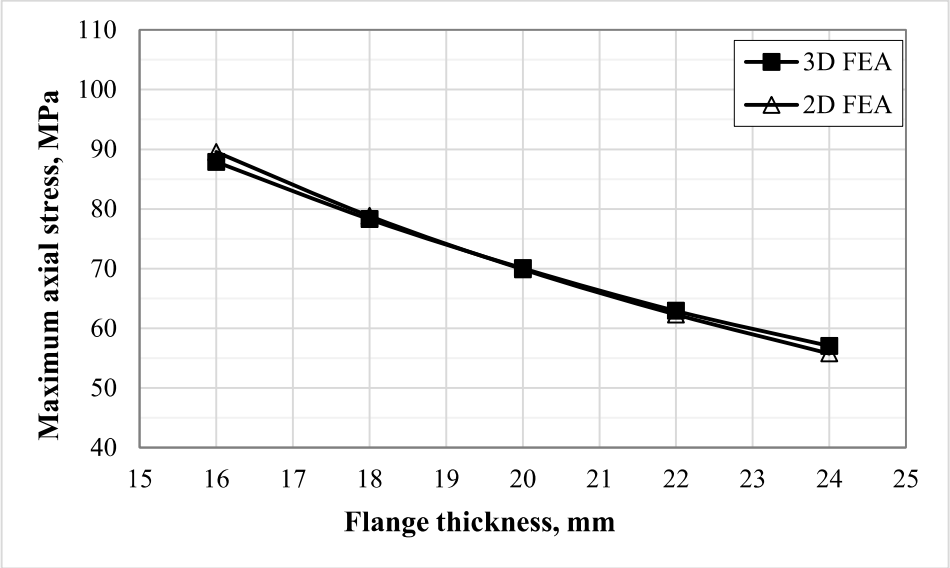

Fig. 14: Maximum axial stress variation with the flange thickness

Maximum hoop stress vs flange thickness, the influence of the flange thickness on the maximum hoop stress has been illustrated in Fig. 15. The maximum hoop stress has been found and measured numerically at the bottom outer surface of the hub and at mid-pint between adjacent bolts. The results show that the maximum hoop stress has been affected by the flange thickness and it has increased when the flange thickness decreased. Decreasing the

flange thickness leads to decrease the flange stiffness. Therefore, the flange bending at the bolt holes are higher than that at the mid-point between any adjacent bolts. This produces high hoop stress at this region due to the applied boundary conditions, which are bolt load and internal pressure. In addition, the results of the 3D FEA are higher that the 2D FEA and this is due to the axisymmetric of the applied bolt loads of the 2D FEA, which were converted to pressure and applied around the flange. This minimize the flange rotation in the hoop direction, so that the 2D FEA results are less than the 3D FEA.

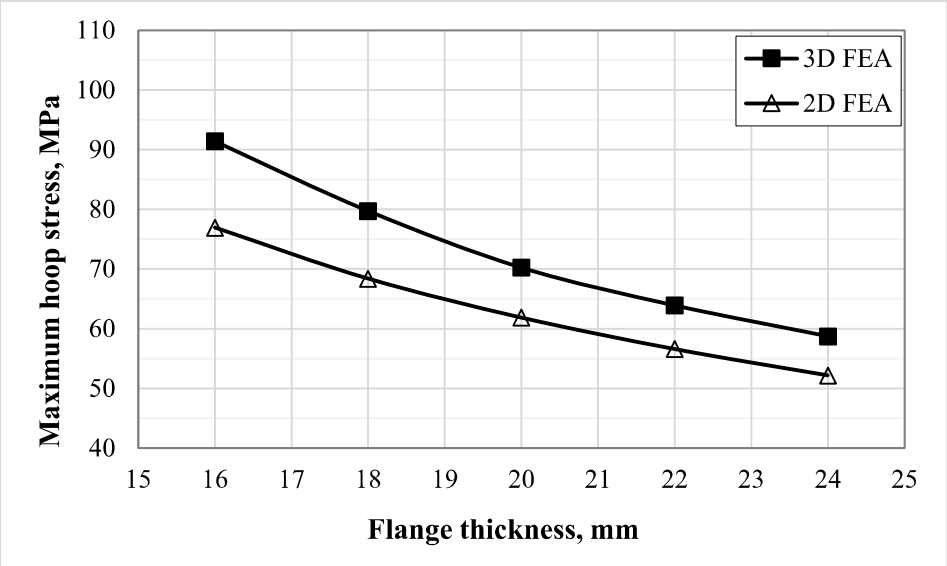

Fig. 15: Maximum hoop stress variation with the flange thickness

Maximum radial stress vs flange thickness, Fig.16 shows the effect of the flange thickness on the maximum radial stress. The maximum radial stress has been found at the top surface of the flange and around the bolt hole. As shown in the figure, decreasing the flange thickness leads to increase the maximum radial stress. This happens because of the flange bending which is produced due to the applied boundary conditions and increases with decreasing the flange thickness.

Fluid pressure penetration vs flange thickness, the distribution of the fluid pressure penetration between the flange and the gasket for different flange thickness using 2D and 3D FEA is illustrated in the Fig. 17. The bolt load is 15 kN and the internal pressure is 8 MPa. The chosen flange thicknesses are 24, 20 and 16 mm. As shown in the results, the leakage propagation in the radial direction increases with decreasing the flange thickness for both 2D and 3D FEA. This occurs due to the decreasing of the flange thickness that makes the flange

more flexible and increase the flange bending. This led to reduce the contact stress between the flange and the gasket thereby increasing development of the fluid pressure penetration. The agreement between the 2D and 3D FEA is excellent

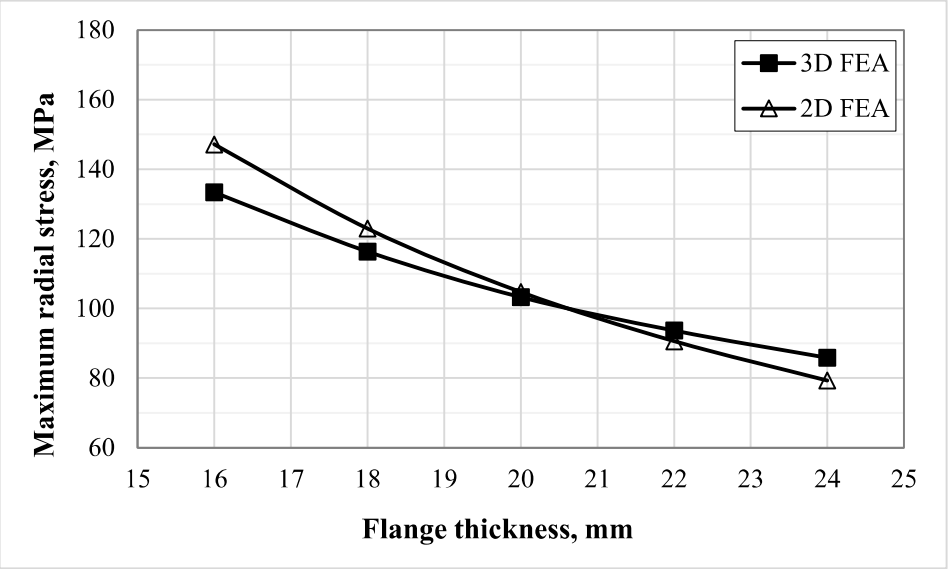

Fig. 16: Maximum radial stress variation with the flange thickness

6.8 Hub thickness effect

The section investigates the effect of the hub thickness at the bottom (HTB) on the maximum stresses in the axial, hoop and radial directions. The range of the hub thickness at the bottom from 25, which is recommended by the standards, to 17 mm.

Maximum axial stress vs hub thickness, Fig. 18 shows the maximum axial stress variation with the hub thickness at the bottom for the 2D and 3D FEA. It seems that the relationship between the maximum stress and the hub thickness is almost linear and reducing the hub thickness leads to increase the maximum axial stress. This due to the reduction in the contact area between the flange disc and the hub and that minimizes the flange strength and increases the flange bending, which leads to increase the axial stress. A good agreement is obtained between the 2D and 3D FEA.

Maximum hoop stress vs hub thickness, the influence of the hub thickness at the bottom on the maximum hoop stress has been illustrated in the Fig. 19 using 2D and 3D FEA. it is noticed that the maximum hoop stress is affected by the hub thickness at the bottom and it increases when the hub thickness decreases. This is due to the increasing of the flange bending because of the reduction in the hub thickness.

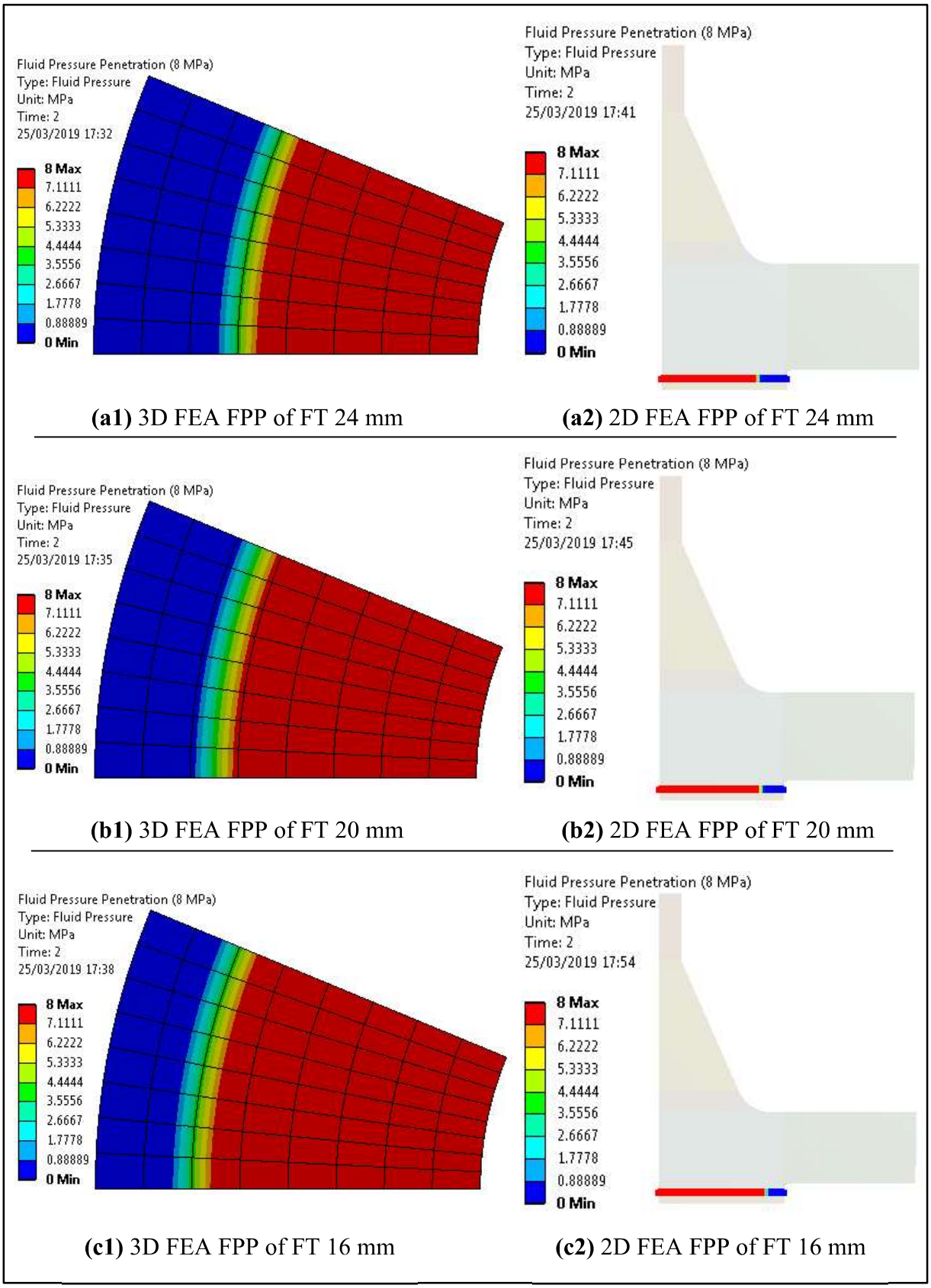

(a1) 3D FEA FPP of FT 24 mm **(a2)** 2D FEA FPP of FT 24 mm

(b1) 3D FEA FPP of FT 20 mm **(b2)** 2D FEA FPP of FT 20 mm

(c1) 3D FEA FPP of FT 16 mm **(c2)** 2D FEA FPP of FT 16 mm

Fig. 17: 2D & 3D FEA fluid pressure penetration variation with the flange thickness

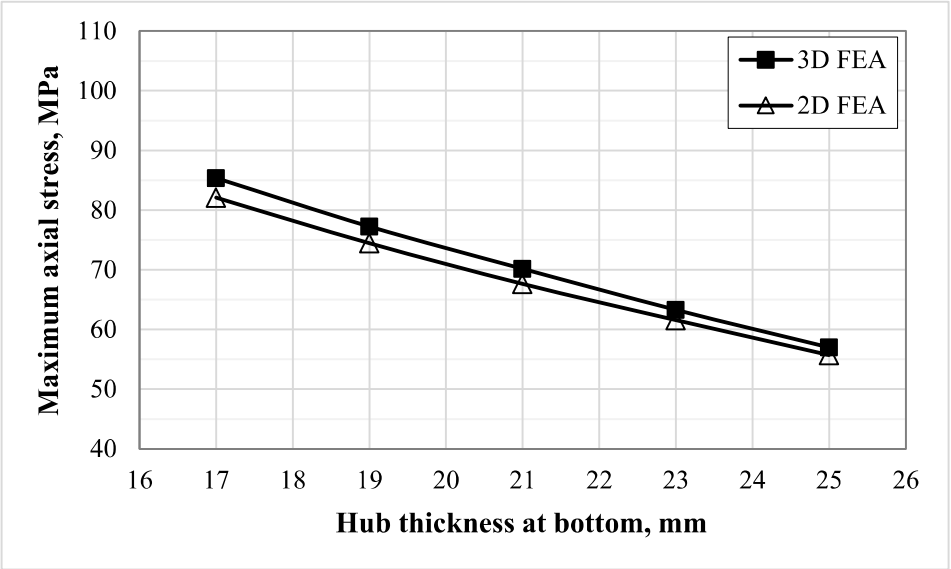

Fig. 18: Maximum axial stress variation with the hub thickness at the bottom

In addition, the results of the 3D FEA is higher than the 2D FEA. This occurs because of that the maximum hoop stress located at the outer surface of the hub and distribution of the bolt load. In the 3D FEA, the bolt force distributed on eight bolt around the flange whereas in the 2D FEA, the bolt force distributed equally around the flange.

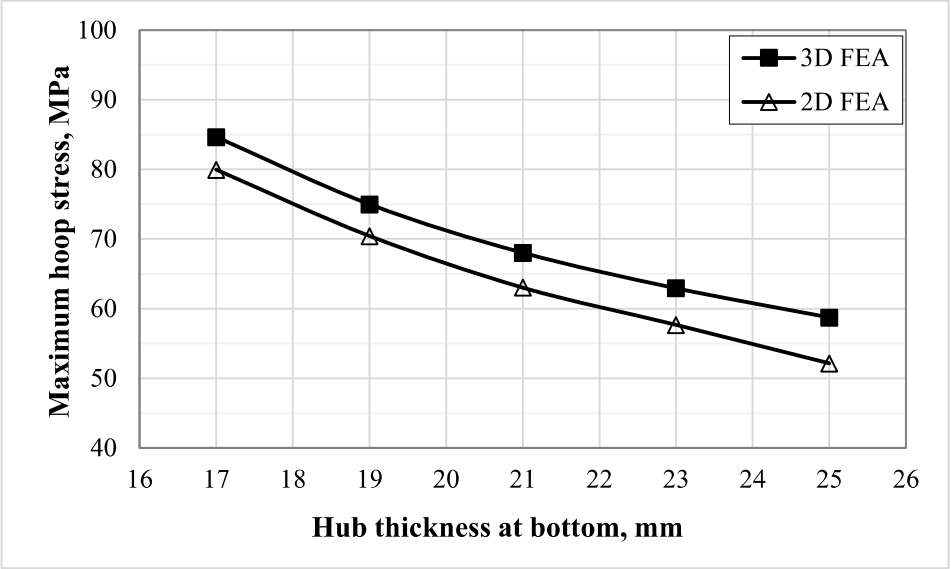

Fig. 19: Maximum hoop stress variation with the hub thickness at the bottom

Maximum radial stress vs hub thickness, Fig. 20 explains the relationship between the maximum radial stress and the hub thickness at the bottom. It seems that the hub thickness has small effect on the maximum radial stress. The 3D FEA shows results higher than the 2D FEA. This happened due to location of the maximum radial stress, which is near the bolt hole, and the difference in the method of applying the bolt load. However, the behaviour and agreement between of the two FEA is still good.

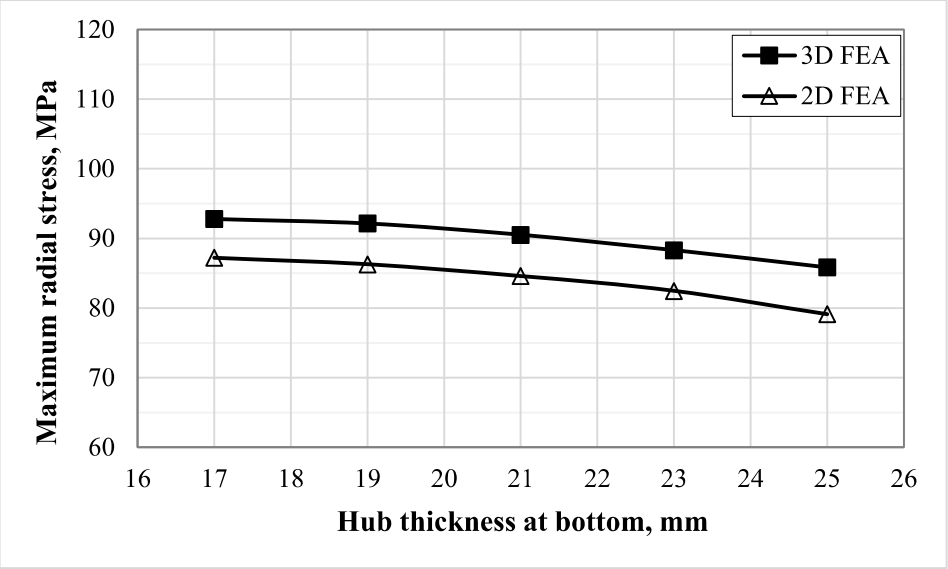

Fig. 20: Maximum radial stress variation with the hub thickness at the bottom

Fluid pressure penetration vs hub thickness, Fig. 21 illustrates the fluid pressure penetration between the flange and the gasket for range of the hub thicknesses (25, 21 and 17 mm). The bolt load is 15 kN and the internal pressure is 8 MPa. As shown in the figure, the leakage propagates more in the radial direction when the hub thickness decreases. This is due to the reduction in the strength of the hub-flange intersection region, which increases the flange bending, thereby, decreasing the contact stress between the flange and the gasket.

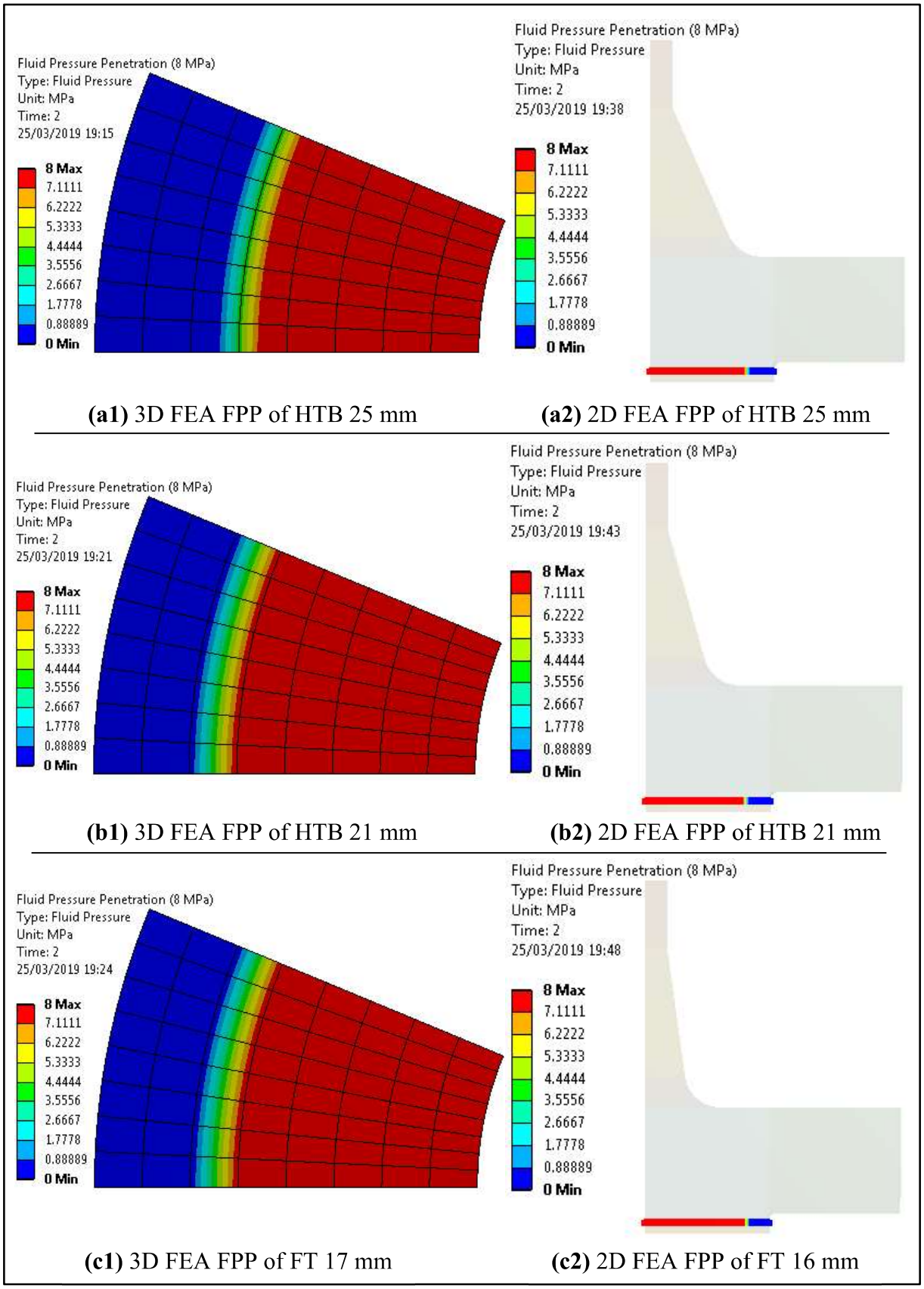

(a1) 3D FEA FPP of HTB 25 mm **(a2)** 2D FEA FPP of HTB 25 mm

(b1) 3D FEA FPP of HTB 21 mm **(b2)** 2D FEA FPP of HTB 21 mm

(c1) 3D FEA FPP of FT 17 mm **(c2)** 2D FEA FPP of FT 16 mm

Fig. 21: 2D & 3D FEA fluid pressure penetration with the hub thickness at the bottom

7. Conclusion

The findings from this study make several contributions to the current literature. First, using finite element analysis, the leakage propagation has been simulated utilizing the PPNC criterion in ANSYS, which gives a good determination of the leakage point. This is difficult to be found by other methods, which are relatively time-consuming and expensive. Thereby, they can be avoided in any applications. Secondly, the simulations have found good agreement between 3D and 2D axisymmetric FEA, so the latter can be used for greater efficiency. Regarding the results, the maximum contact pressure falls more rapidly at higher pressures compared with low pressures. The effect of the bolt load on the leakage point reduces as the internal pressure increases. In addition, the results show that there is a linear relationship between the bolt load and the internal pressure at the leakage. Furthermore, the effect of the flange geometry dimensions (flange thickness and hub thickness) on the leakage development and maximum stresses in axial, hoop and radial directions have been investigated in this study.

Acknowledgements

This work is funded by the Higher Committee for Education Development (HCED) in Iraq, so the authors would like to acknowledge them for their support during the study.

References

1. ASME Boiler and Pressure Vessel Code, Section VIII, Division 2, Appendix 2, *Rules for Bolted Flange Connections with Ring Type Gaskets.,* 2001.
2. Waters EO, R.D., Wesstrom DB, Williams FSG., *Formulas for stresses in bolted flanged connections*., Transactions of the ASME 1937.
3. Waters EO, R.D., Wesstrom DB, Williams FSG., *Development of general formulas for bolted flanges*, Chicago, Illinois: Taylor Forge and Pipe Works; 1949,.
4. Muhsin Aljuboury, Md Jahir Rizve, Stephen Grove, Richard Cullen, *Bolted fibre-reinforced polymer flange joints for pipelines: A review of current practice and future challenges.,* Proceedings of the Institution of Mechanical Engineers, Part L: Journal of Materials: Design and Applications, 2018.

5. Sawa, T., Higurashi, N., and Akagawa, H., *A stress analysis of pipe flange connections.* Journal of Pressure Vessel Technology, 1991, 113(4): p. 497-503.
6. Muhsin Aljuboury, Md Jahir Rizve, Stephen Grove, Richard Cullen, *A numerical investigation of the sealing performance of a bolted GFRP flange joint with rubber gasket*, Eleventh International Conference on Composite Science and Technology, *ICCST/11,* American University of Sharjah, Sharjah, UAE, 4-6 April, 2017.
7. Muhsin Aljuboury, Md Jahir Rizve, Stephen Grove, Richard Cullen, *Bolted flange joint made of glass fibre reinforced polymer (GFRP) for oil and gas pipelines*, Proceedings of the ASME 2018 Pressure Vessels and Piping Conference (PVP2018), Prague, Czech Republic, 15-20 July 2018.
8. Muhsin Aljuboury, Md Jahir Rizve, Stephen Grove, Richard Cullen, *Manufacturing glass fibre reinforced polymer (GFRP) bolted flange connections by using a vacuum infusion process*, in Eleventh International Conference on Composite Science and Technology, ICCST/11, American University of Sharjah, Sharjah, UAE, 4-6 April, 2017.
9. Muhsin Aljuboury, Md Jahir Rizve, Stephen Grove, Richard Cullen, *Stress analysis of bolted FRP flange connections under internal pressure*, *5th PRIMaRE Conference,* Bristol University, Bristol, UK, *5-6 July 2018*..
10. Muhsin Aljuboury, Md Jahir Rizve, Stephen Grove, Richard Cullen, *Development of manufacturing a bolted flange joint from glass fibre braid reinforced polymer using a vacuum infusion process (VIP)*, International Conference on Manufacturing of Advanced Composites (ICMAC 2018), Nottingham University, Nottingham, UK, 10-12 July 2018.
11. Krishna, M. Murali, Shunmugam M. S., and Prasad N. Siva, *A study on the sealing performance of bolted flange joints with gaskets using finite element analysis.* International Journal of Pressure Vessels and Piping, 2007, 84(6): p. 349-357.
12. Shoji, Y. and Nagata S., *Analysis of gasketed flanges with ordinary elements using apdl control,* Toyo Engineering Corporation, Narashino-City, Chiba, Japan.
13. ANSYS User's Manual, *ANSYS Mechanical APDL Technology Demonstration Guide.* Canonsburg, USA, ANSYS Inc, 2013.

14. ANSYS User's Manual, *Contact Technology Guide,.* Canonsburg, USA, ANSYS Inc, 2009.

15. Harris, T., *Implementing Fluid Pressure Penetration.* The Focus, 2009 (71).